Neuron, Vol. 26, 659–670, June, 2000, Copyright ©2000 by Cell Press

Activity Coregulates Quantal AMPA and NMDA Currents at Neocortical Synapses

Alanna J. Watt, Mark C. W. van Rossum, Katrina M. MacLeod, Sacha B. Nelson, and Gina G. Turrigiano*
Department of Biology and
Center for Complex Systems
Brandeis University
Waltham, Massachusetts 02454

Summary

AMPA and NMDA receptors are coexpressed at many central synapses, but the factors that control the ratio of these two receptors are not well understood. We recorded mixed miniature or evoked synaptic currents arising from coactivation of AMPA and NMDA receptors and found that long-lasting changes in activity scaled both currents up and down proportionally through changes in the number of postsynaptic receptors. The ratio of NMDA to AMPA current was similar at different synapses onto the same neuron, and this relationship was preserved following activity-dependent synaptic scaling. These data show that AMPA and NMDA receptors are tightly coregulated by activity at synapses at which they are both expressed and suggest that a mechanism exists to actively maintain a constant receptor ratio across a neuron's synapses.

Introduction

Determining the factors that regulate the number and type of receptors clustered at central synapses is crucial for an understanding of synaptic transmission and plasticity. Most excitatory central synapses coexpress AMPA and NMDA receptors (Bekkers and Stevens, 1989; Jones and Baughman, 1991; McBain and Dingledine, 1992). While AMPA receptors mediate fast excitation, NMDA receptors generate a much slower and longer-lasting current, and, in addition, they flux Ca^{2+}. The relative ratio of these two receptor types at a synapse will therefore profoundly influence the time course and summation of synaptic currents, as well as the amount of Ca^{2+} influx in response to particular patterns of presynaptic activity. This suggests that the ratio of these two receptor types at central synapses should be tightly regulated, but the factors that control this ratio are not well understood.

Early in development, some central synapses contain only NMDA receptors (Isaac et al., 1995, 1997; Liao et al., 1995; Rumpel et al., 1998; Petralia et al., 1999). The rapid insertion of AMPA receptors into these synapses in an NMDA receptor–dependent manner is thought to underlie their maturation (Wu et al., 1996) and has also been proposed as a mechanism for long-term potentiation (LTP) (Isaac et al., 1995, 1997; Liao et al., 1995). Although there is some disagreement over whether LTP and long-term depression (LTD) regulate the amplitude of NMDA currents, the majority of studies report that NMDA currents and the number of NMDA receptors clustered at synaptic sites are unaffected by LTP and LTD protocols (Muller and Lynch, 1988; Bashir et al., 1991; Clark and Collingridge, 1995; Issac et al., 1995; Selig et al., 1995; Carroll et al., 1999). These studies suggest that AMPA and NMDA receptors can be independently regulated over short time scales and suggest that the ratio of AMPA to NMDA current should vary from synapse to synapse.

Synapse-specific forms of synaptic plasticity have long been thought to play an important role in the activity-dependent refinement of central circuits. More recently, it has become clear that mechanisms that regulate the total strength of a neuron's synapses are also important for allowing experience to selectively modify synaptic connections (Bear et al., 1987; Miller, 1996; Davis and Goodman, 1998; Turrigiano, 1999). One important mechanism for controlling synaptic strength allows neurons to slowly scale the AMPA component of excitatory synapses up or down in the right direction to compensate for long-lasting changes in activity (Lissen et al., 1998; O'Brien et al., 1998a; Rutherford et al., 1998; Turrigiano et al., 1998). A number of studies have also suggested that activity may regulate NMDA receptor expression (Audinat et al., 1994; Catalano et al., 1997; Hickmott and Constantine-Paton, 1997), subunit composition (Carmignoto and Vicini, 1992; Scheetz and Constantine-Paton, 1994; Flint et al., 1997; Quinlan et al., 1999), and localization (Rao and Craig, 1997; Liao et al., 1999). This raises the questions of whether NMDA currents are scaled up and down by long-lasting changes in activity, whether this scaling is proportional to the scaling of AMPA currents, and what the relationship is between AMPA and NMDA current at different synapses onto the same neuron.

Here, we used cultured cortical neurons to record from synapses that express both AMPA and NMDA receptors. We recorded miniature excitatory postsynaptic currents (mEPSCs) and excitatory postsynaptic currents (EPSCs) that arose from coactivation of both receptors and found that AMPA and NMDA currents were bidirectionally regulated by long-lasting changes in activity. As demonstrated previously for the AMPA current (O'Brien et al., 1998a; Turrigiano et al., 1998), the change in NMDA current could be accounted for postsynaptically, and noise analysis suggests that NMDA currents were modified through changes in the number of open channels. The regulation of NMDA current occurred without any change in decay kinetics or in the voltage dependence of the Mg^{2+} blockade. The ratio of NMDA to AMPA current was similar from neuron to neuron and was not modified by activity, indicating that activity scaled both currents up or down in a proportional manner. Finally, different synapses onto the same neuron had similar NMDA-to-AMPA ratios, and this relationship was preserved by synaptic scaling. These data suggest that at synapses coexpressing AMPA and NMDA receptors, activity regulates both receptor types in a proportional

*To whom correspondence should be addressed (e-mail: turrigiano@brandeis.edu).

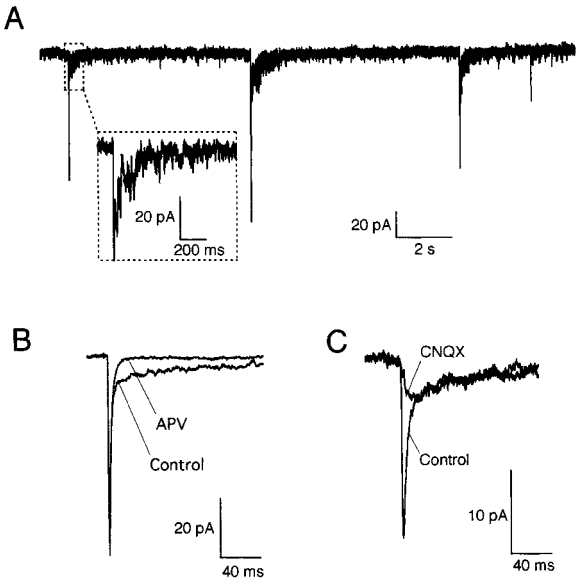

Figure 1. mEPSCs Arising from Coactivation of AMPA and NMDA Receptors

(A) Example of mEPSCs recorded in 0 Mg^{2+} ACSF. Inset shows the slowly decaying NMDA component.

(B) An example of the average mEPSC before and after wash-in of 50 μM APV to block the NMDA current.

(C) An example of the average mEPSC before and after wash-in of 25 μM CNQX to block the AMPA current.

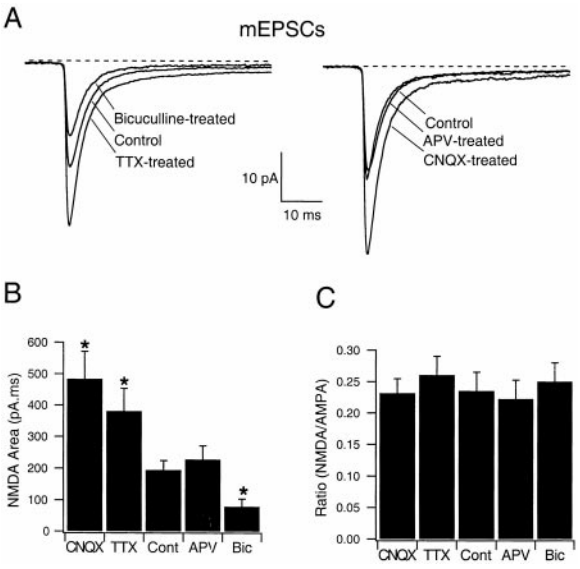

Figure 2. Activity Regulates the Amplitude of Both the AMPA and the NMDA Components of Mixed mEPSCs

(A) Left: average AMPA-NMDA mEPSCs from neurons grown for 2–3 days in either control medium (n = 16) or medium supplemented with TTX (n = 16) or bicuculline (n = 8); right: average AMPA-NMDA mEPSCs from neurons grown for 2 days in either control medium or medium supplemented with CNQX (n = 7) or APV (n = 6).

(B) Area of the NMDA component of the average mEPSC for each neuron was measured and averaged for each treatment condition. NMDA area varied significantly as a function of treatment ($p = 0.0002$, ANOVA; asterisk = significantly different from control, $p < 0.03$, corrected t test).

(C) Ratio of NMDA-to-AMPA current for neurons grown under each condition. There were no significant differences between conditions.

manner, and that a mechanism exists to actively maintain a fixed ratio of NMDA to AMPA receptors at individual neocortical synapses.

Results

Experiments were performed on dissociated cultures from postnatal day 3–5 (P3–P5) rat visual cortex after 7–10 days in vitro or on acute slices from P13–P16 rat visual cortex. Cultures contain both glutamatergic pyramidal neurons and GABAergic interneurons (Rutherford et al., 1997, 1998). Over the first few days in culture, these neurons extend processes, form extensive synaptic interconnections, and become spontaneously active (Rutherford et al., 1997, 1998; Turrigiano et al., 1998). All culture experiments were performed on neurons with a pyramidal morphology (see Experimental Procedures).

Measurement of Mixed AMPA-NMDA mEPSCs

Activity scales the AMPA component of excitatory synaptic strengths up or down by modifying the AMPA quantal amplitude (Turrigiano et al., 1998). To ask whether the NMDA component of mEPSCs changes in parallel with the AMPA component, we recorded mixed mEPSCs arising from activation of both AMPA and NMDA receptors (Figure 1A). To record mixed AMPA-NMDA mEPSCs, we obtained whole-cell recordings from pyramidal neurons in the presence of tetrodotoxin (TTX) (to block spike-mediated release) and bicuculline (to block $GABA_A$-mediated events). After washing out external Mg^{2+}, mEPSCs with two kinetically distinct components were seen: a rapidly rising and decaying AMPA component and a more slowly decaying NMDA component (Figure 1A). The slow component was blocked by amino-phosphono-valeric acid (APV), a selective antagonist of NMDA-type glutamate receptors (Figure 1B), whereas the fast component was blocked by 6-cyano-7-dinitroquinoxaline-2,3-dione (CNQX) a selective antagonist of AMPA/kainate glutamate receptors (Figure 1C). Mixed mEPSCs were detected on the rising phase of the AMPA component of the mEPSC (see Experimental Procedures), so this method will not detect pure NMDA events that would arise from synapses with NMDA but no AMPA receptors.

Since the kinetics of the AMPA and NMDA components of the mEPSC differ dramatically (Edmonds et al., 1995), they can be separated temporally to determine the amplitude or area of each component. Pure AMPA mEPSCs (recorded in the presence of APV) have rise times under one ms, and the average decay time constant is 3.1 ± 0.8 ms (n = 64 neurons). The AMPA component of the mEPSC will therefore decay to <1% of its peak value within 15 ms (Figure 1B), and measurement of pure AMPA events 15 ms after the peak showed that on average, the residual AMPA current was only -0.6 ± 0.3 pA at this time. To assess the rise times of pure NMDA events from our neurons under our recording conditions, we recorded pure NMDA currents (in the presence of CNQX) from synaptically connected pairs

Table 1. Effects of Activity on mEPSC Amplitude and Kinetics

Treatment	AMPA Rise Times (ms)	τ_{NMDA} (ms)	AMPA Amplitude (pA)	NMDA Amplitude (pA)
Control (n = 16)	0.89 ± 0.07	163.7 ± 50.9	−25.5 ± 2.0	−6.0 ± 0.6
TTX (n = 16)	0.84 ± 0.06	149.2 ± 20.2	−38.2 ± 3.5*	−9.2 ± 0.6*
CNQX (n = 7)	0.74 ± 0.07	144.1 ± 21.9	−40.4 ± 3.4*	−9.1 ± 0.8*
Bicuculline (n = 9)	0.95 ± 0.08	135.0 ± 35.3	−17.5 ± 1.0*	−4.5 ± 0.3*
APV (n = 6)	0.74 ± 0.07	157.0 ± 42.5	−28.8 ± 3.6	−6.4 ± 0.5

Average mEPSC rise times, NMDA decay time constants (τ_{NMDA}), and AMPA and NMDA amplitudes for neurons grown under the different experimental conditions. Activity enhancement (bicuculline), deprivation (TTX, CNQX), and NMDA receptor blockade for two days (APV) did not influence the average 20%–80% rise times of mEPSCs (not significantly different, $p = 0.54$). τ_{NMDA} was determined by fitting the decay phase of the slow component of the average mEPSC for each neuron with a single exponential and averaging the values obtained for neurons grown under each condition, and these values were not significantly different between conditions ($p = 0.88$). AMPA and NMDA amplitudes were influenced by the different experimental conditions; asterisk = significantly different from control, $p < 0.03$, corrected t test.

of neurons (n = 3) or measured pure NMDA mEPSCs from recordings with exceptionally low noise levels (n = 3; Figure 1C). The NMDA currents peaked after 15.5 ± 2.5 ms, close to previously reported values (Hestrin et al., 1990; Lester et al., 1990), and the average NMDA amplitude from isolated events was 102.3% ± 4.6% of that obtained from mixed events. Therefore, to measure the amplitude of the NMDA component of mixed mEPSCs largely uncontaminated by AMPA current, the peak current (averaged over 5 ms) was determined in a window between 15 and 25 ms after the AMPA peak. To estimate the error in measurement of the AMPA component of the mixed mEPSCs, mixed mEPSCs were first recorded, and then APV was washed in to allow recording of pure AMPA mEPSCs. Values of the AMPA peak obtained from mixed mEPSCs were 106.5% ± 3.5% of the values obtained from isolated AMPA events (n = 4).

Regulation of Quantal NMDA Currents by Activity

To investigate whether long-term changes in activity regulate the magnitude of quantal NMDA currents, spontaneous activity was increased or decreased for 2–3 days. Activity was blocked by incubating cultures with TTX or enhanced by incubating cultures with bicuculline, which by blocking $GABA_A$-mediated inhibition raises firing rates by a factor of 2–3 (Turrigiano et al., 1998). MEPSCs recorded from individual pyramidal neurons grown under the different conditions were aligned on the rising phase of the AMPA peak and averaged to obtain an average AMPA-NMDA mEPSC for each neuron. Long-lasting changes in activity bidirectionally regulated the amplitude of the AMPA component of the mEPSCs (Figure 2A, left panel), as reported previously (Turrigiano et al., 1998). The NMDA component of the mEPSC was also modified by activity, and in the same direction as the AMPA component: activity-enhancement decreased, whereas activity blockade increased, the quantal NMDA current (Figure 2A, left panel). Blockade of AMPA receptors for two days with CNQX (which largely abolishes spiking activity in these cultures) also significantly increased both components of the mEPSC, while blockade of NMDA receptors for 2 days with APV (which does not significantly influence firing rates) had no significant effect on either component (Figure 2A, right panel).

The area of the NMDA component of the average mEPSC from each neuron was determined by integrating the current between 15 and 500 ms after the peak (a time when the NMDA component had decayed back to baseline for most events). TTX and CNQX treatment increased the NMDA area to 235% ± 37% and 256% ± 43% of control values, respectively. In contrast, bicuculline treatment decreased the NMDA area to 42% ± 13% of control values, while APV had no significant effect on NMDA area (121% ± 21% of control values, control: n = 16, TTX: n = 16, bicuculline: n = 9, CNQX: n = 7, APV: n = 6, p = 0.0002, ANOVA; Figure 2B). This method of measurement underestimates the NMDA area, because it does not include the rising phase of the NMDA current. Consequently, we also calculated the area using an alternative method, in which the decay phase of the average mEPSC from each neuron was fit with a double exponential, and the fast, predominantly AMPA component was subtracted from the average waveform to leave the slow, predominantly NMDA component. This method gave results similar to those shown in Figure 2B and also revealed a significant change in NMDA area as a function of activity.

Activity blockade or enhancement did not significantly influence the passive properties of the neurons, as reported previously (Rutherford et al., 1998; Turrigiano et al., 1998; Desai et al., 1999); there were no significant differences in resting potentials (V_m), input resistances (R_{in}), or whole-cell capacitance between conditions. In addition, these manipulations do not influence the kinetics of AMPA mEPSCs (Rutherford et al., 1998; Turrigiano et al., 1998), and consistent with this, there was no change in AMPA rise times (Table 1). The decay kinetics of the NMDA currents were also unaffected by the experimental conditions (Table 1), suggesting that there were no significant changes in NMDA subunit composition that could influence the kinetics (Carmignoto and Vicini, 1992; Flint et al., 1997).

The Average NMDA-to-AMPA Ratio of mEPSCs Is Not Influenced by Changes in Activity

Like the NMDA area, the amplitudes of the AMPA and NMDA components of the mEPSCs were also significantly modified by activity. Amplitudes were measured for each individual mEPSC, and these were then averaged to determine a value for each neuron. Both the AMPA and NMDA amplitudes were significantly increased by TTX or CNQX treatment, were unaffected

by APV treatment, and were significantly decreased by bicuculline treatment (Table 1). To ask whether the ratio of NMDA to AMPA amplitudes remained constant after the different treatments, we determined the NMDA-to-AMPA ratio for each individual mEPSC and obtained an average ratio for each neuron. For control neurons, the NMDA-to-AMPA ratio was 0.23 ± 0.03. The ratio of NMDA to AMPA did not change significantly following activity blockade or enhancement, indicating that the average amplitudes of the AMPA and NMDA components of the mEPSCs are regulated proportionally by activity ($p = 0.78$, ANOVA; Figure 2C). Similar results were obtained by first averaging all mEPSCs from a given neuron and then measuring the peak AMPA and NMDA current from the average mEPSC: TTX significantly increased both AMPA and NMDA amplitudes (to 157% ± 18% and 168% ± 21% of control values, respectively), and bicucilline significantly decreased both amplitudes (to 71% ± 5% and 68% ± 8% of control values, respectively). The NMDA-to-AMPA ratio measured in this way was also not significantly modified by activity (TTX was 107% ± 14% of control values, and bicuculline was 95% ± 5% of control values).

Synaptic Scaling Does Not Modify the NMDA-to-AMPA Ratio of Evoked Synaptic Currents

TTX treatment scales up the AMPA amplitude of evoked synaptic currents, as well as that of mEPSCs (Turrigiano et al., 1998). To determine whether the AMPA and NMDA components of evoked currents are scaled proportionally, cultures were treated with TTX for 2 days, and recordings were obtained between pairs of synaptically connected pyramidal neurons (Figure 3A). On average, both the AMPA and NMDA components of the evoked EPSCs (measured at −50 mV in low Mg^{2+}) from TTX-treated cultures were increased almost 3-fold relative to control cultures ($n = 6$ pairs in each condition, TTX significantly different from control, $p = 0.004$ for AMPA and 0.014 for NMDA, Student's t test; Figure 3B). The ratio of AMPA to NMDA current remained constant as synaptic currents were scaled up ($p = 0.98$, Student's t test; Figure 3B). The increase in amplitude of EPSCs following activity blockade is somewhat larger (a 2- to 3-fold increase; Figure 3; Turrigiano et al., 1998) than is the increase in mEPSCs (a 1.6- to 2-fold increase; Table 1; Rutherford et al., 1998; Turrigiano et al., 1998). This difference may be due to the use of an amplitude cutoff for detecting mEPSCs, because when small control events that are just below the amplitude cutoff are scaled up by activity blockade, they will tend to skew the TTX distribution toward smaller values and reduce the apparent change in amplitude.

Activity Regulates the Postsynaptic Sensitivity to Glutamate

We have shown previously that changes in the AMPA quantal amplitude are accompanied by changes in the postsynaptic sensitivity to glutamate (Turrigiano et al., 1998). To ask whether changes in the NMDA component of the mEPSCs can also be accounted for postsynaptically, we examined the response of pyramidal neurons to applied glutamate in artificial cerebrospinal fluid (ACSF) containing 2 mM Mg^{2+} and 20 μM CNQX to block

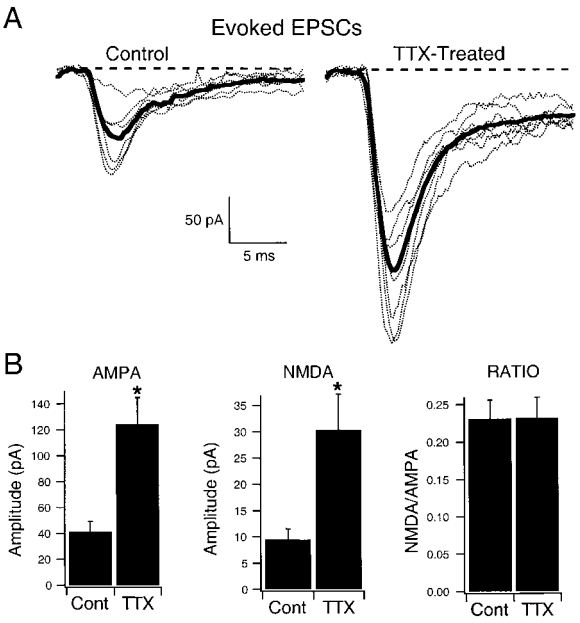

Figure 3. Spike-Mediated Transmission between Pairs of Monosynaptically Connected Pyramidal Neurons

(A) Example of paired recording (postsynaptic neuron voltage clamped at −50 mV in 0.1 mM Mg^{2+}) from control neurons or neurons grown in TTX for 2 days. Dotted lines indicate individual trials, and solid lines indicate the average of many trials. Dashed lines indicate baseline.

(B) Average amplitude of the AMPA (left) and NMDA (center) components of the EPSC from control or TTX-treated neurons, and the ratio of NMDA to AMPA current under the two conditions (right, $n = 6$ pairs in each condition). Both the AMPA and NMDA amplitude are significantly increased by TTX treatment ($p < 0.02$), while the ratio is unaffected ($p = 0.98$).

AMPA/kainate currents. Neurons were voltage clamped to potentials between −80 and +50 mV, and NMDA-mediated currents were elicited by brief puffs of glutamate from a patch pipette (50 μM for 5 ms; Figure 4A). A voltage-dependent current was elicited that reversed close to 0 mV and could be completely blocked by the selective NMDA receptor antagonist MK-801. In neurons that had been activity deprived for 48 hr, these NMDA receptor–mediated glutamate-evoked currents were approximately twice the amplitude of those from control neurons (values are significantly different for all voltages, control: $n = 13$, TTX: $n = 16$, Student's t test; Figure 4A). Measurement of the glutamate-evoked current at different positions along the apical-like dendrite demonstrated that there was an ∼2-fold increase in NMDA current from TTX-treated neurons at all locations tested (Figure 4B). This increase is comparable to that measured previously for AMPA currents following activity blockade (Turrigiano et al., 1998). This increase in glutamate-evoked current is unlikely to result from changes in extrasynaptic receptors, because at this developmental stage in vitro, the glutamate responsiveness of cortical and hippocampal neurons is primarily localized to synaptic "hot spots," and estimates suggest that <5%–25% of receptors are extrasynaptic (Jones and Baughman, 1991; Rosenmund et al., 1995; Liu et al., 1999).

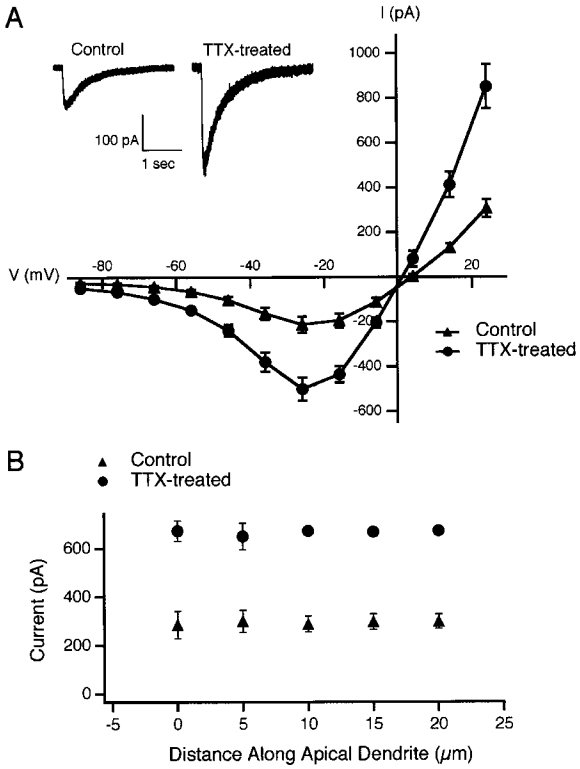

Figure 4. Activity Blockade Increases the Amplitude of NMDA Receptor–Mediated Currents Elicited by Postsynaptic Glutamate Application

(A) Example traces of the response of a control and a TTX-treated neuron from sister cultures to a brief puff of glutamate to the proximal dendrites and soma (voltage clamped to −40 mV). Recordings were obtained in ACSF containing 2 mM Mg^{2+}. The I–V curve shows the peak current for control (triangles, n = 13) and TTX-treated (circles, n = 16) neurons. TTX was significantly different from control at all voltages ($p < 0.05$, Student's t test).

(B) NMDA receptor–mediated currents elicited from control and TTX-treated neurons by the application of glutamate to various sites along the apical-like dendrites. TTX was significantly different from control at all sites (n = 4 neurons in each condition, $p \leq 0.01$, Student's t test).

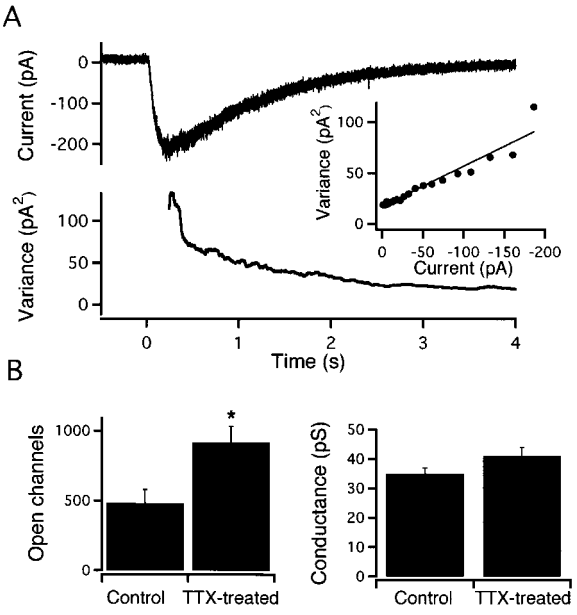

Figure 5. Noise Analysis of Glutamate-Evoked NMDA Currents

(A) Top: an example of NMDA receptor–mediated current evoked by a 5 ms puff of glutamate. Bottom: the variance during the decay phase of the current shown in the top trace. Inset: a straight line fit of the variance versus the current.

(B) Estimated number of open channels (left) and single channel conductance (right) using stationary noise analysis of glutamate-evoked currents in control and sister TTX-treated neurons. TTX treatment increases by ~2-fold the number of open channels ($p = 0.009$). The single channel conductance of the NMDA receptor–mediated current was not significantly affected by TTX treatment.

When recording in the presence of Mg^{2+}, NMDA currents are reduced in amplitude due to a partial, voltage-dependent Mg^{2+} block (Mayer et al., 1984). The resulting current is well described by the following equation:

$$I = \frac{g(V - V_{rev})}{1 + \frac{[Mg]}{k} e^{(-V/V_0)}},$$

where g is the total unblocked NMDA conductance, V_{rev} is the reversal potential of the NMDA current, k is a binding constant for Mg^{2+}, and V_0 is the voltage dependence of this binding (Jahr and Stevens, 1990). Fits of the NMDA current–voltage (I–V) curves for control and TTX-treated neurons yielded values for V_{rev} (2.2 ± 0.6 mV), k (15 ± 5 mM), and V_0 (12.8 ± 1.2 mV) that were not significantly different between conditions, indicating that the reversal potential and the voltage dependence of the Mg^{2+} block were not affected by activity blockade. In contrast, TTX treatment significantly increased the total conductance, g, to 240% of control values, indicating that either the number or the unitary conductance of NMDA receptors increased in response to prolonged activity blockade.

Stationary Noise Analysis of Glutamate-Evoked Currents

The increased amplitude of postsynaptic currents elicited by glutamate application could be due to an increase in channel number or a change in the single channel conductance. To differentiate between these possibilities, we performed a fluctuation analysis of the glutamate-evoked NMDA currents. Because these currents decayed very slowly relative to single channel fluctuations (Figure 5A, top panel), the data can be treated as stationary (Jonas and Sakmann, 1992). Data from one 5 ms application of glutamate is shown in Figure 5A, top panel. At the peak of the current, the variance was high, as expected, and then decreased as the current decayed back to baseline and the number of open channels decreased (Figure 5A, bottom panel). A plot of the variance against the current during the decay phase was well fit by a straight line (Figure 5A, inset), and an estimate of the single channel conductance can be derived from the slope of this line (Anderson and Stevens, 1973; Jonas and Sakmann, 1992).

For control neurons, the estimated single channel conductance after correcting for the Mg^{2+} block was

35 ± 2 pS (n = 13). The estimated single channel conductance for TTX-treated neurons was slightly higher, 41 ± 3 pS (n = 16), but this difference was not significant (p = 0.065). These values agree well with other estimates of the NMDA receptor single channel conductance (40–50 pS), derived from patch-clamp recordings or fluctuation analysis (Robinson et al., 1991; Spruston et al., 1995). The major difference between control and TTX currents was in the number of open channels, which approximately doubled from 482 ± 99 to 917 ± 115 (TTX significantly different from control, p = 0.009; Figure 5B). These data strongly suggest that activity regulates the amplitude of NMDA currents by modifying the number of postsynaptic NMDA receptors.

Ratio of NMDA to AMPA Current at Individual Synapses from Pyramidal Neurons in Culture and Slice

As described above, the ratio of NMDA to AMPA current averaged across all mEPSCs recorded from a given neuron is not influenced by the history of activity of the neuron (Figure 2C), indicating that the average amplitudes of the NMDA and AMPA currents change in parallel. But how tightly correlated is the relationship between the AMPA and NMDA amplitudes at individual synapses? To investigate this, the AMPA amplitude was plotted against the NMDA amplitude for each mEPSC recorded from a given neuron, and the correlation coefficient was determined. Four examples are shown in Figure 6A, two from control neurons (left) and two from TTX-treated neurons (right). For all four neurons, there was a strong correlation between the two amplitudes, and across our entire data set (for neurons with an average NMDA component larger than 2 pA, control: n = 11, TTX: n = 16), the correlation coefficient ranged from 0.41 to 0.92 (TTX: average, r = 0.67 ± 0.04, control: average, r = 0.60 ± 0.03). Occasionally, large AMPA events with negligible NMDA components were observed, but such events were rare (Figure 6).

To assess the uniformity of the NMDA–AMPA relationship across neurons, we randomly selected 30 events from each neuron and again plotted the AMPA amplitude against the NMDA amplitude. For control neurons, the correlation coefficient was 0.72, and for TTX-treated neurons, it was 0.78 (Figure 6B). Both slopes were significantly different from zero (p = 0.0001), and the slopes and intercepts were similar to each other for the two conditions (control: slope = 2.55, intercept = −6.5; TTX-treated: slope = 2.65, intercept = −5.4). These data suggest that as long-term changes in activity modify the strength of a neuron's synapses, the relationship between the AMPA and NMDA amplitudes at individual synapses is preserved.

Electrotonic filtering is unlikely to introduce a significant amount of correlation between AMPA and NMDA amplitudes, because rapid AMPA currents will be much more filtered than will slow NMDA currents (Spruston et al., 1993), so filtering will not reduce both components of the mEPSC proportionally. To directly assess the effects of electrotonic filtering on the degree of correlation, the correlations obtained for the fastest events (those with rise times faster than 0.7 ms) were compared with those obtained from the entire population of events (n = 3 neurons). The correlation coefficients were not different for the two populations of events: the correlation coefficients obtained for the fastest events were 103% ± 3% of the values obtained for the entire population, suggesting that electrotonic filtering is not introducing a significant degree of correlation between NMDA and AMPA amplitudes.

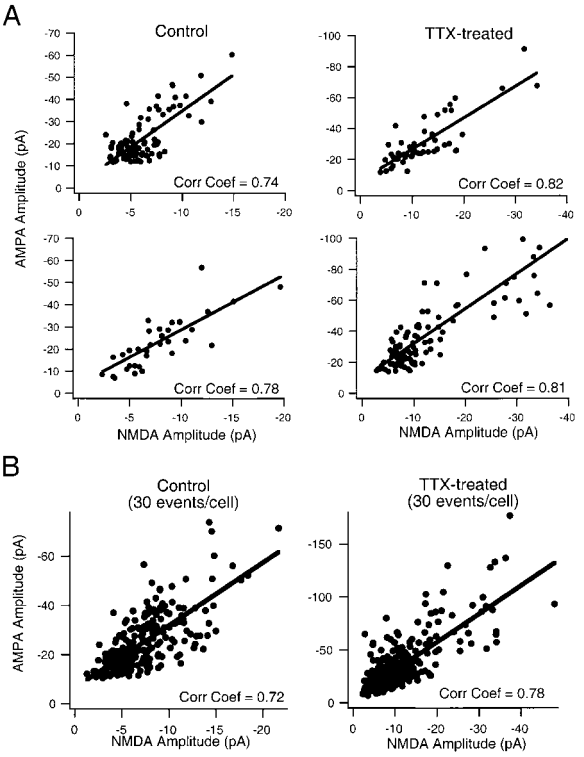

Figure 6. The Amplitudes of the NMDA and AMPA Components of Individual mEPSCs Are Highly Correlated for Both Control and Activity-Deprived Neurons in Cortical Cultures

(A) AMPA versus NMDA peak amplitudes plotted for each mEPSC from four example neurons. Left: data from two control neurons; right: data from two TTX-treated neurons. Solid line is the best straight line fit, and the correlation coefficients for each fit are indicated.

(B) Thirty mEPSCs were randomly selected from each control (n = 11) or TTX-treated (n = 16) neuron, and the AMPA versus NMDA peak amplitudes plotted. Solid line is the best straight line fit, and the correlation coefficients for each fit are indicated. Both slopes are significantly different from zero, p = 0.0001.

To determine whether a similar relationship between NMDA and AMPA currents exists in cortical neurons that have not been dissociated, whole-cell recordings were obtained from neurons in layer 4 of P13–P16 rat visual cortical slices. An example is shown in Figure 7A, in which AMPA mEPSCs were first recorded in 2 mM Mg^{2+}, and the Mg^{2+} was then washed out to reveal the large NMDA component. The average NMDA-to-AMPA ratio was 0.41 ± 0.03 for these neurons (n = 6). Plotting the AMPA against the NMDA amplitude for individual mEPSCs revealed a degree of correlation similar to that seen for pyramidal neurons in culture (Figure 7B); the correlation coefficient ranged from 0.37 to 0.91, and on average was 0.65 ± 0.05 (n = 6).

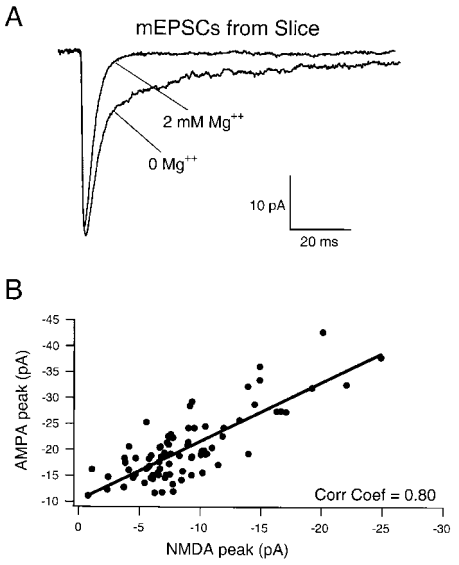

Figure 7. The Amplitudes of the NMDA and AMPA Components of Individual mEPSCs Recorded from Layer 4 Neurons from Visual Cortical Slices Are Highly Correlated

(A) Average mEPSC from a layer IV neuron recorded in ACSF containing 2 mM Mg^{2+}, showing a fast AMPA component only. Washing in Mg^{2+}-free ACSF revealed the slower NMDA component of the average mEPSC.

(B) AMPA versus NMDA peak amplitudes plotted for each mEPSC from a layer IV pyramidal neuron. Solid line is the best straight line fit, and the correlation coefficient was 0.80.

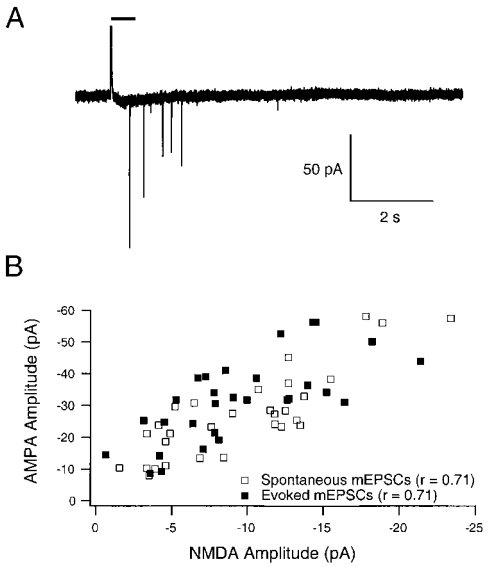

Figure 8. Comparison of the NMDA-to-AMPA Ratio from a Small and a Large Number of Synapses

(A) Representative recording of mEPSCs evoked from one or a few synapses using focal application of 0.5 M sucrose. The pressure artifact marks the beginning of a 400 ms pulse of sucrose (dark bar) that evoked a burst of mEPSCs.

(B) Plot of NMDA amplitude against AMPA amplitude for sucrose-evoked events ("Evoked mEPSCs") and spontaneous events ("Spontaneous mEPSCs") from the same neuron.

Variability in the NMDA-to-AMPA Ratio from Individual Release Sites

Two factors that could generate a significant correlation between AMPA and NMDA amplitudes across a neuron's synapses are (1) variations in glutamate concentration from vesicle to vesicle, and (2) covariance in the number of AMPA and NMDA receptors across synapses. Variations in vesicle diameter introduce a significant variability in mEPSC amplitude at one or a few release sites (Bekkers et al., 1990; Frerking et al., 1995; Forti et al., 1997). If this variability were large enough (and assuming that neither AMPA nor NMDA receptors are saturated), then it would introduce some correlation between AMPA and NMDA currents from mEPSCs occurring randomly at many release sites, even if the ratio of receptors were different at each site, because large vesicles would evoke larger AMPA and NMDA currents, and smaller vesicles would evoke smaller AMPA and NMDA currents. However, the correlation should degrade as more and more synapses with different NMDA-to-AMPA ratios are sampled from.

To compare the correlation between AMPA and NMDA amplitudes from a small and a large number of synapses, we used focal application of sucrose to elicit mixed AMPA-NMDA mEPSCs from a restricted population of synapses. For each neuron, we compared these to the mEPSCs arising spontaneously from a large number of synapses. When a patch pipette filled with sucrose was moved along a segment of the proximal apical-like dendrite, hot spots could be located where ejection of hypertonic sucrose evoked a burst of mEPSCs (Figure 8A). These responses were quite localized, as movement of the pipette by a few micrometers in either direction along the dendrite abolished the response. All data were collected from hot spots within 40 μm of the soma to reduced differences in electrotonic filtering. These mEPSCs probably arise from one to several synaptic sites (Bekkers et al., 1990; Liu and Tsien, 1995; Forti et al., 1997; Liu et al., 1999). There was significant variation in mEPSC amplitudes evoked from a single hot spot, presumably due to variations in transmitter content from vesicle to vesicle (Figure 8).

When the AMPA amplitude was plotted against the NMDA amplitude for mEPSCs evoked from a hot spot, a strong correlation was present. The NMDA-to-AMPA ratio for large mEPSCs was similar to that for small mEPSCs (Figure 8B), indicating that there was little saturation of either AMPA or NMDA currents for large events, as demonstrated by several recent studies (Liu and Tsien, 1995; Liu et al., 1999; Mainen et al., 1999; Umemiya et al., 1999). Similar results have been reported for mEPSCs from cultured cortical neurons arising from single identified synaptic sites (Umemiya et al., 1999) and for evoked EPSCs from cortical slice (Stern et al., 1992). The degree of correlation for mEPSCs evoked from a hot spot was very similar to that obtained from spontaneous mEPSCs originating from many different synaptic sites onto the same neuron (Figure 8B); the average correlation coefficient for evoked mEPSCs was 0.63 $\pm$ 0.03, and for spontaneous mEPSCs was 0.65 $\pm$ 0.03 (not significantly different, $n = 6$ neurons, $p = 0.53$, paired t test). These data demonstrate that the degree of correlation between AMPA and NMDA currents does not

degrade as the number of synapses sampled from increases, suggesting that the correlation across synapses cannot be accounted for by variations in glutamate concentration from vesicle to vesicle.

A Constant Ratio of NMDA to AMPA Current across a Neuron's Synapses

The strong correlation between the amplitudes of the AMPA and NMDA components of mEPSCs from different synapses could arise because the ratio of receptors is relatively constant from synapse to synapse. One approach to determining if the NMDA-to-AMPA ratio is similar or different across synapses is to compare the mean and the variance of the NMDA-to-AMPA ratio at a small number of synaptic sites with those from the entire population of synapses (Figure 9A). If the ratio of receptors is similar at every synapse, then the ratio at any randomly selected synaptic site should be very close to the average ratio for the neuron. In keeping with this, the average NMDA-to-AMPA ratios obtained from hot spots (0.24 $\pm$ 0.03) were very similar to those obtained from the spontaneous events arising from many synaptic sites onto the same neurons (0.26 $\pm$ 0.02, n = 6; Figure 9B). In addition, sampling from many synapses with similar ratios should generate a distribution of ratios that is only slightly broader than the distribution from one or a few sites (Figure 9A, right). In contrast, if the ratio of receptors is different at different synaptic sites, then sampling from many sites should generate a distribution of ratios that is significantly broader than that obtained at any one site (Figure 9A, left).

A convenient measure of the broadness of a distribution is the coefficient of variation (CV), defined as the standard deviation divided by the mean. The CV of the ratio of NMDA to AMPA current evoked from hot spots was close to that for spontaneous mEPSCs (not significantly different, evoked: CV = 0.42 $\pm$ 0.03, spontaneous: CV = 0.39 $\pm$ 0.02, n = 6, p = 0.27, paired t test; Figures 9C and 9D), as expected if the NMDA-to-AMPA ratio was similar across synapses. In contrast, the CV of the AMPA amplitudes should be larger for random events arising from many sites than for events evoked from hot spots, because there is significant variation in the number of AMPA receptors across synapses. As expected, the CV of the AMPA amplitudes from spontaneous events arising randomly from many different synaptic sites (0.53 $\pm$ 0.05) was greater than the CV of events evoked from a hot spot (0.40 $\pm$ 0.04, significantly different, n = 6, p = 0.01, paired t test; Figure 9E). These values for the CV of the AMPA amplitudes are similar to those obtained by comparing loose-patch recordings from single boutons to randomly arising mEPSCs (Forti et al., 1997). Taken together, these data strongly suggest that there is little variability in the ratio of NMDA to AMPA receptors across a neuron's synapses.

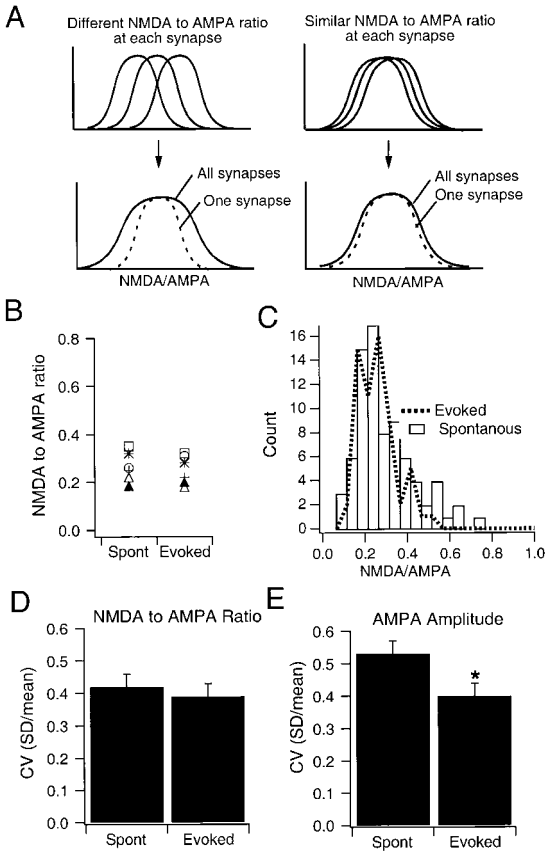

Figure 9. Comparison of the Mean and Variability of the NMDA-to-AMPA Ratio from a Small and a Large Number of Synapses

(A) Cartoon illustrating the effects of sampling from synapses with similar or different NMDA-to-AMPA ratios. The distribution of NMDA-to-AMPA ratios is illustrated for three neurons with similar (upper right) or different (upper left) mean ratios. If the ratios at each synapse are different, then sampling from many synapses will generate a distribution that is broader (lower left, "All synapses") than that from a single synapse (lower left, "One synapse"). On the other hand, if the ratio is similar at different sites (upper right), then sampling from many synapses will generate a distribution that is similar to that from a single synapse (lower right).

(B) Comparison of the ratio of NMDA to AMPA current for sucrose-evoked or spontaneous mEPSCs for each of six different neurons. Each symbol represents the average NMDA-to-AMPA ratio for spontaneous events arising from many different synapses (left) and events evoked from a hot spot (right) for an individual neuron.

(C) Histogram showing the distribution of NMDA-to-AMPA ratios for individual mEPSCs from an example neuron. Dashed line indicates mEPSCs evoked from a small number of synapses with focal applications of hypertonic sucrose, while bars indicate spontaneously occurring mEPSCs from a large number of synapses.

(D) The average CV (standard deviation divided by the mean) for the NMDA-to-AMPA ratios for evoked and spontaneous mEPSCs. The CVs are not significantly different (n = 6, p = 0.27, paired t test).

(E) The CVs of the AMPA amplitude for spontaneous and evoked events are significantly different (n = 6, p = 0.015, paired t test).

Discussion

Our data demonstrate that long-lasting changes in activity modify the quantal amplitude of AMPA and NMDA currents in a coordinated manner. Both the AMPA and NMDA components of mEPSCs are increased proportionally by activity blockade and decreased proportionally by activity enhancement. In addition, there is a strong correlation between the amplitudes of the AMPA and NMDA components of individual mEPSCs, and this correlation is preserved when synaptic strengths are

scaled up by activity blockade. These data suggest that the number of AMPA and NMDA receptors at individual synapses is tightly coregulated to maintain a fixed ratio of AMPA to NMDA current.

The activity-dependent regulation of both the AMPA and NMDA components of the mEPSC is likely to occur through postsynaptic changes in the number of receptors clustered at excitatory synapses. Activity blockade increases the amplitude of both AMPA (O'Brien et al., 1998a; Turrigiano et al., 1998) and NMDA receptor–mediated currents (Figure 4) elicited by direct application of glutamate. It has recently been shown that activity-dependent changes in AMPA mEPSC amplitude are accompanied by changes in the intensity of AMPA receptor staining at synaptic sites (O'Brien et al., 1998a), and here we use noise analysis of NMDA currents to demonstrate that the increase in NMDA currents produced by activity blockade can be accounted for by changes in the number of open channels. Taken together, these studies suggest that activity scales mEPSCs up and down by increasing or decreasing the number of postsynaptic AMPA and NMDA receptors, although we cannot rule out additional presynaptic changes that could contribute to the change in AMPA and NMDA synaptic currents.

A striking finding of the present study is the strong correlation between the amplitudes of the AMPA and the NMDA components of individual mEPSCs from both cultured neurons and neurons from visual cortical slices. Because the mean and variability of the NMDA-to-AMPA ratio from a large number of synapses are similar to those from one or a few synapses onto the same neuron, our data strongly suggest that the variability in this ratio from synapse to synapse is small. Conclusions similar to ours were reported recently in a study using Ca^{2+} imaging to identify mixed mEPSCs arising from identified release sites (Umemiya et al., 1999). Interestingly, even when mEPSCs are recorded at one or a few synapses, the correlation coefficient is similar to that obtained from the entire population of active synapses, suggesting that much of the variability in the NMDA-to-AMPA ratio arises from trial-to-trial variability in the ratio of receptors that open at individual synapses. This variability could be due to a number of factors, including trial-to-trial differences in the clearance of glutamate from the synaptic cleft, differential inactivation of AMPA and NMDA receptors, or variability in the NMDA current due to the stochastic opening and closing of a small number of high conductance channels. In addition to suggesting that the ratio of NMDA to AMPA receptors is conserved across synaptic sites, our data show that this relationship remains constant following synaptic scaling, indicating that this ratio is actively maintained in the face of large changes in synaptic strength.

Electrophysiological recordings have consistently found that most (on the order of 70%–80%) of the excitatory synapses on cortical and hippocampal neurons express both AMPA and NMDA receptors (Bekkers and Stevens, 1989; Jones and Baughman, 1991; McBain and Dingledine, 1992; Umemiya et al., 1999) and that by P10, in cortex, "silent" NMDA-alone synapses are largely gone (Isaac et al., 1997; Rumpel et al., 1998). In contrast, immunohistochemical studies on the localization of AMPA and NMDA receptor subunits in hippocampal cultures have found that large numbers of anatomically identified synapses express exclusively one or the other receptor and that the degree of colocalization may be as low as 30% (Rao and Craig, 1997; Lissen et al., 1998; Liao et al., 1999). Furthermore, prolonged changes in activity in hippocampal cultures have been reported to modify the number of immunohistochemically identified sites that express NMDA but not AMPA receptors (Rao and Craig, 1997), or AMPA but not NMDA receptors (Lissen et al., 1998), while a recent study reports that selective blockade of AMPA or NMDA receptors increases the number of AMPA- or NMDA-containing synaptic sites, respectively (Liao et al., 1999). While the results of these studies differ in detail, they have all concluded that the number of sites expressing AMPA and NMDA receptors are independently regulated by activity. Since we recorded only from synapses that express AMPA receptors, our data do not address the issue of whether activity modifies the percentage of synapses that colocalize AMPA and NMDA receptors. What our data do show is that when AMPA and NMDA receptors are colocalized at cortical synapses, the ratio of the two receptors is under tight control, and activity-dependent scaling produces a coordinated and proportional change in both.

A current model of synapse maturation suggests that local activation of NMDA receptors at silent (NMDA-alone) synapses through coincident pre- and postsynaptic activity leads to the insertion of AMPA receptors and the formation of functional synapses (Wu et al., 1996; Constantine-Paton and Cline, 1998). One possibility for how a relatively constant ratio of NMDA to AMPA receptors could be set up and maintained at synapses is if the number of surface AMPA receptors were proportional to the local Ca^{2+} signal generated by NMDA receptor activation. This model seems unlikely because blockade of NMDA receptors does not influence the NMDA-to-AMPA ratio, indicating that this ratio can be maintained in the absence of NMDA receptor signaling. An alternative possibility is that AMPA receptors are inserted into binding sites that are already present in a fixed stochiometry relative to NMDA receptor binding sites. Both AMPA and NMDA receptors are clustered at synapses through interactions with multiple PDZ domain–containing scaffolding proteins (Kornau et al., 1997; O'Brien et al., 1998b). A stochiometric relationship between these AMPA and NMDA receptor scaffolding proteins could explain both the fixed ratio across synaptic sites and the proportional scaling of AMPA and NMDA currents by long-lasting changes in activity.

An intriguing question is how a fixed ratio of AMPA and NMDA receptors can be maintained in the face of ongoing LTP and LTD. Our slice recordings were made between P13 and P16, the developmental period when cortical LTP is most pronounced (Kirkwood et al., 1995). Most models of synaptic plasticity suggest that the currents through AMPA and NMDA receptors are regulated independently by LTP and LTD, which would lead to a divergence in the ratio of NMDA to AMPA current over time. Independent regulation of NMDA and AMPA receptors could account for some of the scatter in the

relationship between NMDA and AMPA amplitudes observed, but the high degree of correlation suggests either that the magnitude of independent regulation is limited or that some mechanism acts over a longer time scale to return the AMPA and NMDA ratios back to their initial values.

Why should NMDA and AMPA currents have a relatively constant ratio at cortical synapses? One possibility is that, since a significant portion of cortical excitation is mediated through NMDA receptors (Nelson and Sur, 1992; Daw et al., 1993), both components of excitation need to change in parallel in order to effectively modify the strength of a synapse. Regulating both receptor types together may also provide an efficient means of stabilizing synaptic strengths during development. In visual cortex, activity can modify the ability of a stimulus to elicit LTP or LTD, and it has been proposed that this could arise from changes in NMDA receptor function (Bear et al., 1987; Bear, 1995; Kirkwood et al., 1996). Ca^{2+} influx through NMDA receptors is necessary for both LTP and some forms of LTD, and it has been hypothesized that the direction of change in synaptic strength is determined by the amount of this influx (Lisman, 1989; Cummings et al., 1996; Hansel et al., 1997; Zucker, 1999). Changes in the number of NMDA receptors could therefore have a profound effect on whether a particular pattern of activity leads to synaptic weakening or strengthening. When neurons scale down NMDA currents in response to a rise in activity, this should favor depression and reduce synaptic strengths. Conversely, when neurons scale up NMDA currents in response to a drop in activity, this should favor potentiation and increase synaptic strengths. Scaling of NMDA currents may thus act synergistically with scaling of AMPA currents to stabilize synaptic strengths. Finally, coupling between the AMPA and NMDA current at individual synapses may provide a means for amplifying and preserving strong synapses while depressing weaker synapses, because a similar level of pre- and postsynaptic correlation will result in more Ca^{2+} influx at synapses with more AMPA and NMDA receptors. This suggests that coregulation of AMPA and NMDA receptors could enhance competition between synapses while at the same time stabilizing the total synaptic strength of the neuron.

Experimental Procedures

Cultures were prepared as previously described (Rutherford et al., 1997; Turrigiano et al., 1998; Desai et al., 1999), except that for some experiments, cultures were maintained in astrocyte-conditioned serum-free medium containing B27 supplement (GIBCO). Briefly, visual cortical cultures were prepared from P3–P5 rat pups, and whole-cell recordings were obtained in ACSF (see below). Experiments were performed after 7–10 days in vitro. All data were obtained in parallel on treated and age-matched sister control cultures. Recordings were obtained from neurons identified morphologically as pyramidal neurons by the teardrop-shaped somata and the presence of an apical-like dendrite. Neurons with this morphology are GABA negative and have pyramidal-like firing patterns (Rutherford et al., 1997, 1998; Turrigiano et al., 1998; Desai et al., 1999), and they make excitatory glutamatergic connections onto other neurons: in more than 50 synaptically connected pairs in which the presynaptic neuron was identified morphologically as pyramidal and the type of synaptic connection was then verified by either the kinetics and reversal potential or pharmacology, only two neurons (<4%) were misidentified. To block activity, cultures were treated with 1 μM TTX, and to raise activity, cultures were treated with 20 μM bicuculline, for 2–3 days. To block AMPA or NMDA receptors, cultures were treated with 50 μM CNQX or 100 μM D-APV, respectively, for 2 days. All drugs were refreshed after 24 hr.

Whole-cell voltage-clamp recordings were obtained using an Axopatch 1D, 1B, or 200B at room temperature as previously described (Rutherford et al., 1997, 1998; Turrigiano et al., 1998). Liquid junction potentials were measured to be 5–6 mV, and voltages were left uncompensated for the junction potential, except for the determination of NMDA I–V curves. Recordings with V_ms above −50 mV, series resistances (R_s) >20 MΩ, R_{in} <200 MΩ, or fewer than 30 mEPSCs were excluded. R_s and R_{in} were continuously monitored throughout data collection, and neurons in which these parameters changed by more than 10% were excluded. Average V_m was −64 ± 1.2 mV, R_{in} was 484 ± 32 MΩ, whole-cell capacitance (WCC) was 34.0 ± 1.7 pF, and R_s was 9.0 ± 0.3 MΩ, and there were no significant differences in any of these parameters between conditions. To record mEPSCs, neurons were held in voltage clamp at −70 mV using an Axopatch 1B or 1D in the presence of TTX (1 μM) and bicuculline (20 μM). In-house software was used to detect and measure mEPSCs; detection criteria included AMPA amplitudes >10 pA and 20%–80% rise times <3 ms; multiple events that overlapped or events with poor baselines were excluded. The amplitude cutoff used here is higher than that used previously to detect pure AMPA mEPSCs (5 pA), because in 0 Mg^{2+}, recordings tended to be noisier than in regular ACSF. In three neurons with low noise, we compared the NMDA-to-AMPA ratio from very small events (between 5 and 10 pA) with that from events with large amplitudes (>10 pA) and found that the ratios were not significantly different (0.30 ± 0.04 for small and 0.32 ± 0.04 for large events), suggesting that the small events do not arise from a fundamentally different pool of synapses. To generate the average mEPSC for each neuron, all events recorded from that neuron were aligned on the rising phase of the AMPA component and averaged. To generate the average mEPSC for a given experimental condition, the average mEPSCs for each neuron recorded in that condition were averaged. Paired recordings were obtained in ACSF with 0.1 mM Mg^{2+}. Spikes were elicited in the presynaptic neuron with depolarizing current pulses while voltage clamping the postsynaptic neuron to various potentials. EPSCs time-locked to the presynaptic spike were detected and aligned relative to the peak of the presynaptic spike. Monosynaptic connections had latencies of <4 ms and <1 ms of jitter in the onset of the EPSC. Traces contaminated by polysynaptic inputs or spontaneous EPSCs were excluded. All data are reported as mean ± SEM for the number of neurons indicated. Unless otherwise noted, statistical comparisons were performed using one-way ANOVAs followed by unpaired two-tailed t tests using a Bonferoni correction factor for multiple comparisons; $p \leq 0.05$ was considered significant.

To determine the postsynaptic responsiveness to glutamate, a picospritzer was used to deliver 5 ms puffs of 50 μM glutamate (using puffer pipettes of 1.5 μm in diameter) to the proximal dendrites and soma while holding pyramidal neurons at a variety of voltages in whole-cell voltage clamp. Series resistance compensation of 70%–80% was used for these experiments. To facilitate voltage clamping at depolarized voltages, $CsMeSO_4$ was used in place of $KMeSO_4$, and the concentration of EGTA was increased to 10 mM in the pipette solution. At least five interleaved repetitions at each voltage were obtained, and the results averaged. To focally deliver hypertonic sucrose, pipettes were filled with 0.5 M sucrose in 0 Mg^{2+} ACSF, and a picospritzer was used at 5 PSI to deliver puffs of 100–400 ms in duration.

To perform noise analysis on glutamate-evoked currents, the mean and variance were calculated for adjacent 200 ms intervals during the decay phase of the glutamate-evoked currents. The decay phase of this current was well fit by a double exponential. To minimize contributions from the decay of the average current, the variance was calculated after subtracting this double exponential fit. The variance of the current was linear in the mean, indicating that only a small fraction of the available channels opened. The unitary conductance was then estimated from the slope of the mean–variance relation. NMDA currents were corrected for the Mg^{2+} block to obtain the conductance in the absence of Mg^{2+}. As the blocking and unblocking kinetics of Mg^{2+} are very fast (Jahr and Stevens, 1990), fluctuations from this process are largely filtered

out, and, as a result, only the mean current will be affected by the block. The effect of the Mg^{2+} block on the mean current was calculated from the I–V curve as described in the Results. For each neuron, the unitary conductance and maximum number of open channels were calculated for five holding potentials (−50, −40, −30, −20, and −10 mV); very similar values were obtained at each potential, so these values were averaged.

Coronal slices containing primary visual cortex were obtained from Long-Evans rats, aged P13–P16, and visualized patch recordings were obtained as previously described (Varela et al., 1999). Animals were deeply anesthetized with isofluorane and decapitated, and their brains were quickly removed and placed in chilled ACSF (5°C). Slices of 400 μm thickness were cut on a vibratome. Slices were maintained at room temperature on semipermeable membranes (Falcon 3090) covered by a thin layer of ACSF continuously oxygenated with 95% O_2/5% CO_2. Slices equilibrated for 1–2 hr prior to recording and remained viable for up to 16 hr. They were transferred one at a time to a submerged chamber mounted on a fixed stage upright microscope and slowly warmed to 34°C–36°C. Slices were superfused with warmed, oxygenated ACSF at a rate of 2–3 ml/min. Slices were transilluminated to permit visualization of the location of primary visual cortex and the boundaries of layer 4. Recordings were obtained from layer 4 neurons with V_m more negative than −60 mV, R_s <20 MΩ, and R_{in} >200 MΩ. The average V_m was −63.4 ± 1.2 mV, R_{in} was 378 ± 62 MΩ, WCC was 36.5 ± 5.7 pF, and R_s was 9.5 ± 1.1 MΩ. Pipette solutions were as reported below, except that 1 mM BAPTA was used in place of the EGTA. MEPSCs were recorded and analyzed as described for cultured neurons.

The solutions were as follows. ACSF contained (in mM): NaCl, 126; KCl, 3; $MgSO_4$, 2; NaH_2PO_4, 1; $NaHCO_3$, 25; $CaCl_2$, 2; and dextrose, 14, and 20 μM glycine; the pH was buffered to 7.4 by bubbling continuously with 5% CO_2/95% O_2. For 0 Mg^{2+} ACSF, the Mg^{2+} was replaced with additional dextrose. For some experiments, glycine was omitted from the ACSF; no difference in the amplitude of NMDA currents was observed with or without glycine, so data from the two conditions were pooled. The internal pipette solution contained (in mM): $KMeSO_4$, 130; KCl, 10; HEPES/K-HEPES, 10; $MgSO_4$, 2; EGTA, 0.5; and ATP, 3; the pH was adjusted to 7.4 with KOH; for some experiments, 100 mM K-gluconate + 20 mM KCl was used instead of $KMeSO_4$.

Acknowledgments

We thank Steven Erat for the preparation of cultures. This research was supported by National Institutes of Health grants K02 NS01893 (G. G. T.), R01 NS36853 (G. G. T.), and RO1 EY11116 (S. B. N.), and by the Sloan Foundation. G. G. T. is an Alfred P. Sloan Fellow.

Received February 24, 2000; revised April 13, 2000.

References

Anderson, C.R., and Stevens, C.F. (1973). Voltage clamp analysis of acetylcholine produced end-plate current fluctuations at frog neuromuscular junction. J. Physiol. *235*, 655–691.

Audinat, E., Lambolex, B., Rossier, J., and Crepel, F. (1994). Activity-dependent regulation of NMDA receptor subunit expression in rat cerebellar granule cells. Eur. J. Neurosci. *6*, 1792–1800.

Bashir, Z.L., Alford, S., Davies, S.N., Randall, A.D., and Collingridge, G.L. (1991). Long-term potentiation of NMDA receptor–mediated synaptic transmission in the hippocampus. Nature *349*, 156–158.

Bear, M.F. (1995). Mechanism for a sliding synaptic modification threshold. Neuron *15*, 1–4.

Bear, M.F., Cooper, L.N., and Ebner, F.F. (1987). A physiological basis for a theory of synapse modification. Science *237*, 42–48.

Bekkers, J.M., and Stevens, C.F. (1989). NMDA and non-NMDA receptors are co-localized at individual excitatory synapses in cultured rat hippocampus. Nature *341*, 230–233.

Bekkers, J.M., Richerson, G.B., and Stevens, C.F. (1990). Origin of variability in quantal size in cultured hippocampal neurons and hippocampal slices. Proc. Natl. Acad. Sci. USA *87*, 5359–5362.

Carmignoto, G., and Vicini, S. (1992). Activity-dependent decrease in NMDA receptor responses during development of the visual cortex. Science *258*, 1007–1011.

Carroll, R.C., Lissen, D.V., von Zastrow, M., Nicoll, R.A., and Malenka, R.C. (1999). Rapid redistribution of glutamate receptors contributes to long-term depression in hippocampal cultures. Nat. Neurosci. *2*, 454–460.

Catalano, S.M., Chang, C.K., and Shatz, C.J. (1997). Activity-dependent regulation of NMDAR1 immunoreactivity in the developing visual cortex. J. Neurosci. *17*, 8376–8390.

Clark, K.A., and Collingridge, G.L. (1995). Evidence that presynaptic changes are involved in the expression of LTP and LTD of NMDA receptor–mediated EPSCs in area CA1 of the hippocampus. J. Physiol. (Paris) *482*, 39–52.

Constantine-Paton, M., and Cline, H.T. (1998). LTP and activity-dependent synaptogenesis: the more alike they are, the more different they become. Curr. Opin. Neurobiol. *8*, 139–148.

Cummings, J.A., Mulkey, R.M., Nicoll, R.A., and Malenka, R.C. (1996). Calcium signaling requirements for long-term depression in the hippocampus. Neuron *16*, 825–833.

Davis, G.W., and Goodman, C.S. (1998). Genetic analysis of synaptic development and plasticity: homeostatic regulation of synaptic efficacy. Curr. Opin. Neurobiol. *8*, 149–156.

Daw, N.W., Stein, P.S.G., and Fox, K. (1993). The role of NMDA receptors in information processing. Annu. Rev. Neurosci. *16*, 207–222.

Desai, N.S., Rutherford, L.C., and Turrigiano, G.G. (1999). Plasticity in the intrinsic excitability of neocortical pyramidal neurons. Nat. Neurosci. *2*, 515–520.

Edmonds, B., Gibb, A.J., and Colquhoun, D. (1995). Mechanisms of activation of glutamate receptor and the time course of excitatory synaptic currents. Annu. Rev. Physiol. *57*, 495–519.

Flint, A.C., Maisch, U.S., Weishaupt, J.H., Kriegstein, A.R., and Monyer, H. (1997). NR2A subunit expression shortens NMDA receptor synaptic currents in developing neocortex. J. Neurosci. *17*, 2469–2476.

Forti, L., Bossi, M., Bergamaschi, A.V., and Malgaroli, A. (1997). Loose-patch recordings of single quanta at individual hippocampal synapses. Nature *388*, 874–878.

Frerking, M., Borges, S., and Wilson, M. (1995). Variation in GABA mini amplitude is the consequence of variation in transmitter concentration. Neuron *15*, 885–895.

Hansel, C., Artola, A., and Singer, W. (1997). Relation between dendritic Ca^{2+} levels and the polarity of synaptic long-term modifications in rat visual cortex neurons. Eur. J. Neurosci. *9*, 2309–2322.

Hestrin, S., Sah, P., and Nicoll, R.A. (1990). Mechanisms generating the time course of dual component excitatory synaptic currents recorded in hippocampal slices. Neuron *5*, 247–253.

Hickmott, P.W., and Constantine-Paton, M. (1997). Experimental down-regulation of the NMDA channel associated with synapse pruning. J. Neurophysiol. *78*, 1096–1107.

Isaac, J.T.R., Nicoll, R.A., and Malenka, R.C. (1995). Evidence for silent synapses: implications for the expression of LTP. Neuron *15*, 427–434.

Isaac, J.T.R., Crair, M.C., Nicoll, R.A., and Malenka, R.C. (1997). Silent synapses during development of thalamocortical inputs. Neuron *18*, 269–280.

Jahr, C.E., and Stevens, C.F. (1990). A quantitative description of NMDA receptor–channel kinetic behavior. J. Neurosci. *10*, 1830–1837.

Jonas, P., and Sakmann, B. (1992). Glutamate receptor channels in isolated patches from CA1 and CA3 pyramidal cells of rat hippocampal slices. J. Physiol. *455*, 143–171.

Jones, K.A., and Baughman, R.W. (1991). Both NMDA and non-NMDA subtypes of glutamate receptor are concentrated at synapses on cerebral cortical neurons in culture. Neuron *7*, 593–603.

Kirkwood, A., Lee, H.-K., and Bear, M.F. (1995). Co-regulation of long-term potentiation and experience-dependent synaptic plasticity in visual cortex by age and experience. Nature *375*, 328–331.

Kirkwood, A., Rioult, M.G., and Bear, M.F. (1996). Experience-dependent modification of synaptic plasticity in visual cortex. Nature *381*, 526–528.

Kornau, H.-C., Seeburg, P.H., and Kennedy, M.B. (1997). Interaction of ion channels and receptors with PDZ domain proteins. Curr. Opin. Neurobiol. *7*, 368–373.

Lester, R.A.J., Clements, J.D., Westbrook, G.L., and Jahr, C.E. (1990). Channel kinetics determine the time course of NMDA receptor–mediated synaptic currents. Nature *346*, 565–567.

Liao, D., Hessler, N.A., and Malinow, R. (1995). Activation of postsynaptically silent synapses during pairing-induced LTP in CA1 region of hippocampal slice. Nature *375*, 400–404.

Liao, D., Zhang, X., O'Brien, R.O., Ehlers, M.D., and Huganir, R.L. (1999). Regulation of morphological postsynaptic silent synapses in developing hippocampal neurons. Nat. Neurosci. *2*, 37–43.

Lisman, J. (1989). A mechanism for the Hebb and the anti-Hebb processes underlying learning and memory. Proc. Natl. Acad. Sci. USA *86*, 9574–9578.

Lissen, D.V., Comperts, S.N., Carroll, R.C., Christine, C.W., Kalman, D., Kitamura, M., Hardy, S., Nicoll, R.A., Malenka, R.C., and von Zastrow, M. (1998). Activity differentially regulates the surface expression of synaptic AMPA and NMDA glutamate receptors. Proc. Natl. Acad. Sci. USA *95*, 7097–7102.

Liu, G., and Tsien, R.W. (1995). Properties of synaptic transmission at single hippocampal synaptic boutons. Nature *375*, 404–408.

Liu, G., Choi, S., and Tsien, R.W. (1999). Variability of neurotransmitter concentration and nonsaturation of postsynaptic AMPA receptors at synapses in hippocampal cultures and slices. Neuron *22*, 395–409.

Mainen, Z.F., Malinow, R., and Svoboda, K. (1999). Synaptic calcium transients in single spines indicate that NMDA receptors are not saturated. Nature *399*, 51–55.

Mayer, M.L., Westbrook, G.L., and Guthrie, P.B. (1984). Voltage-dependent block by Mg^{2+} of NMDA responses in spinal cord neurones. Nature *309*, 261–263.

McBain, C., and Dingledine, R. (1992). Dual-component miniature excitatory synaptic currents in rat hippocampal CA3 pyramidal neurons. J. Neurophysiol. *68*, 16–27.

Miller, K.D. (1996). Synaptic economics: competition and cooperation in synaptic plasticity. Neuron *17*, 371–374.

Muller, D., and Lynch, G. (1988). Long-term potentiation differentially affects two components of synaptic responses in hippocampus. Proc. Natl. Acad. Sci. USA *85*, 9346–9350.

Nelson, S.B., and Sur, M. (1992). NMDA receptors in sensory information processing. Curr. Opin. Biol. *2*, 484–488.

O'Brien, R.J., Kambol, S., Ehlers, M.D., Rosen, K.R., Kischback, G.D., and Huganir, R.L. (1998a). Activity-dependent modulation of synaptic AMPA receptor accumulation. Neuron *21*, 1067–1078.

O'Brien, R.J., Lau, L.G., and Huganir, R.L. (1998b). Molecular mechanisms of glutamate receptor clustering at excitatory synapses. Curr. Opin. Neurobiol. *8*, 364–369.

Petralia, R.S., Esteban, J.A., Wang, Y.-X., Partridge, J.G., Zhao, H.-M., Wenthold, R.J., and Malinow, R. (1999). Selective acquisition of AMPA receptors over postnatal development suggests a molecular basis for silent synapses. Nat. Neurosci. *2*, 31–36.

Quinlan, E.M., Philpot, B.D., Huganir, R.L., and Bear, M.F. (1999). Rapid, experience-dependent expression of synaptic NMDA receptors in visual cortex in vivo. Nat. Neurosci. *2*, 352–357.

Rao, A., and Craig, A.M. (1997). Activity regulates the synaptic localization of the NMDA receptor in hippocampal neurons. Neuron *19*, 801–812.

Robinson, H.P.C., Sahara, Y., and Kawai, N. (1991). Nonstationary fluctuation analysis and direct resolution of single channel currents at postsynaptic sites. Biophys. J. *59*, 295–304.

Rosenmund, C., Feltz, A., and Westbrook, G.L. (1995). Synaptic NMDA receptor channels have a low open probability. J. Neurosci. *15*, 2788–2795.

Rumpel, S., Hatt, H., and Gottmann, K. (1998). Silent syapses in the developing rat visual cortex: evidence for postsynaptic expression of synaptic plasticity. J. Neurosci. *18*, 8863–8874.

Rutherford, L.C., DeWan, A., Lauer, H., and Turrigiano, G.G. (1997). BDNF mediates the activity-dependent regulation of inhibition in neocortical cultures. J. Neurosci. *17*, 4527–4535.

Rutherford, L.C., Nelson, S.B., and Turrigiano, G.G. (1998). Opposite effects of BDNF on the quantal amplitude of pyramidal and interneuron excitatory synapses. Neuron *21*, 521–530.

Scheetz, A.J., and Constantine-Paton, M. (1994). Modulation of NMDA receptor function: implications for vertebrate neural development. FASEB J. *8*, 745–752.

Selig, D.K., Hjelmstad, G.O., Herron, C., Nicoll, R.A., and Malenka, R.C. (1995). Independent mechanisms for long-term depression of AMPA and NMDA responses. Neuron *15*, 417–426.

Spruston, N., Jaffe, D.B., Williams, S.H., and Johnston, D. (1993). Voltage- and space-clamp errors associated with the measurement of electrotonically remote synaptic events. J. Neurophysiol. *70*, 781–802.

Spruston, N., Jonas, P., and Sakmann, B. (1995). Dendritic glutamate receptor channels in rat hippocampal CA3 and CA1 pyramidal neurons. J. Physiol. *482*, 325–352.

Stern, P., Edwards, F.A., and Sakmann, B. (1992). Fast and slow components of unitary EPSCs on stellate cells elicited by focal stimulation in slices of rat visual cortex. J. Physiol. *449*, 247–278.

Turrigiano, G.G. (1999). Homeostatic plasticity in neuronal networks: the more things change, the more they stay the same. Trends Neurosci. *22*, 221–228.

Turrigiano, G.G., Leslie, K.R., Desai, N.S., Rutherford, L.C., and Nelson, S.B. (1998). Activity-dependent scaling of quantal amplitude in neocortical neurons. Nature *391*, 892–895.

Umemiya, M., Senda, M., and Murphy, T.H. (1999). Behavior of NMDA and AMPA receptor–mediated miniature EPSCs at rat cortical neuron synapses identified by calcium imaging. J. Physiol. *521*, 113–122.

Varela, J.A., Song, S., Turrigiano, G.G., and Nelson, S.B. (1999). Differential depression at excitatory and inhibitory synapses in visual cortex. J. Neurosci. *19*, 4293–4304.

Wu, G.-Y., Malinow, R., and Cline, H.T. (1996). Maturation of a central glutamatergic synapse. Science *274*, 972–976.

Zucker, R.S. (1999). Calcium- and activity-dependent synaptic plasticity. Curr. Opin. Neurobiol. *9*, 305–313.